

SUPPLEMENTAL MATERIAL

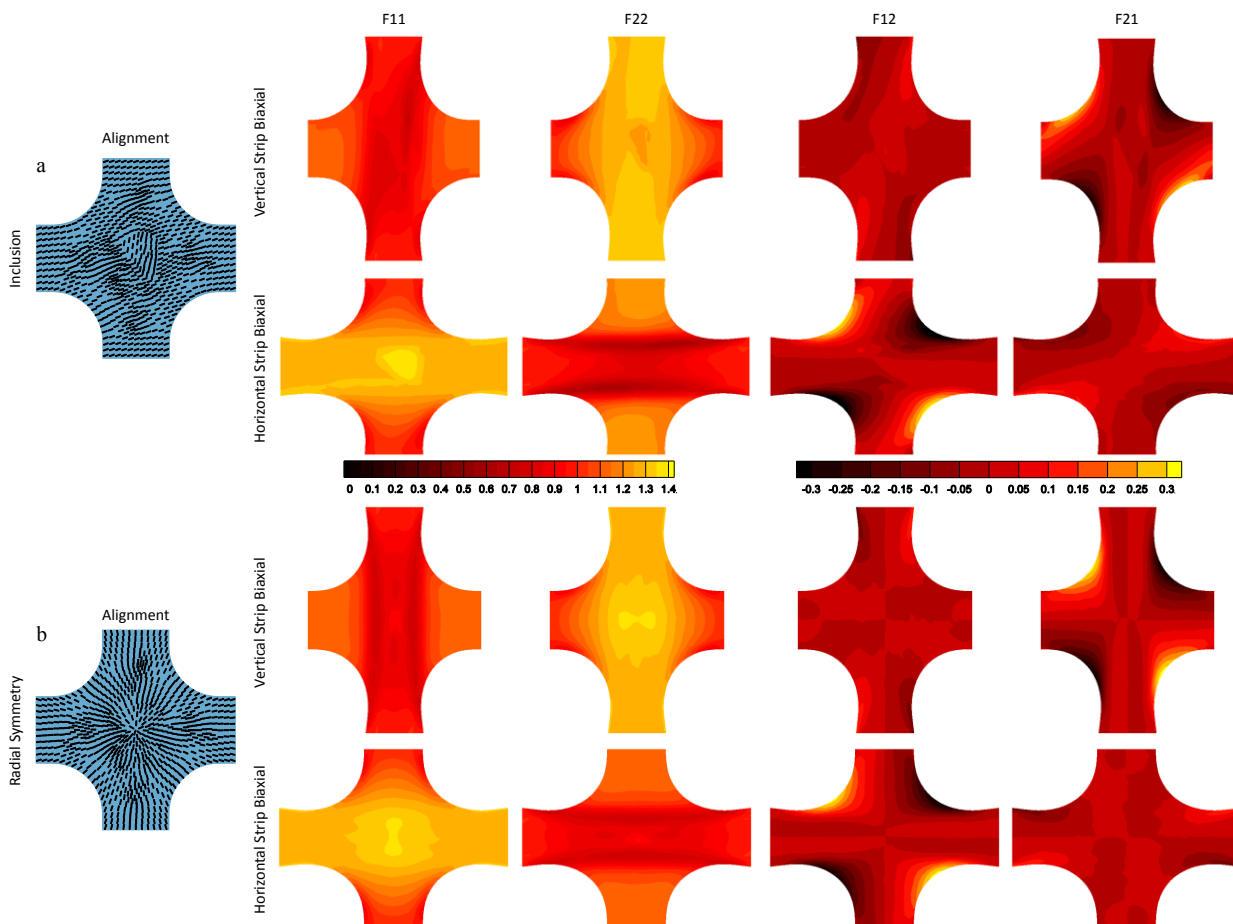


Fig. S1: Fiber alignment and full-field deformation gradient tensor components for strip biaxial extensions of (a) simulated sample with inclusion for which the inclusion varies only in prescribed fiber orientation ( $80^\circ$  vs.  $20^\circ$ ) and (b) simulated radially symmetric sample for which the prescribed fiber orientation varied.

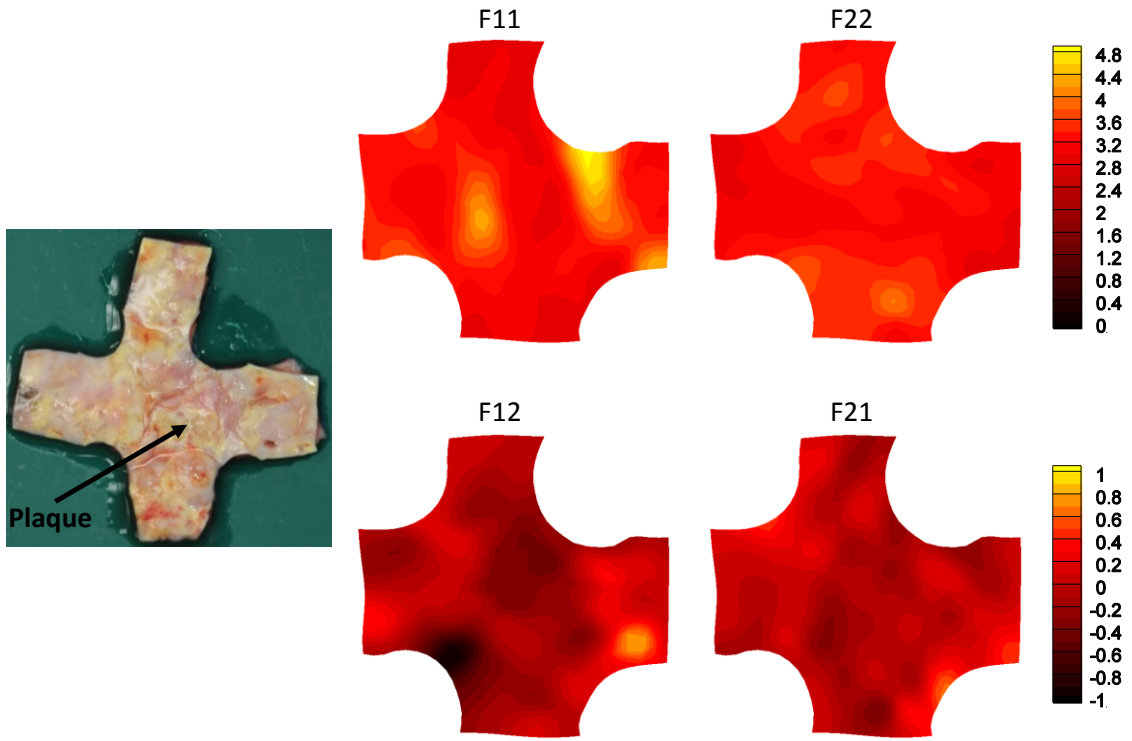


Fig. S2: Full-field deformation gradient tensor components for equibiaxial extension of aortic sample containing a large arteriosclerotic transmural plaque.

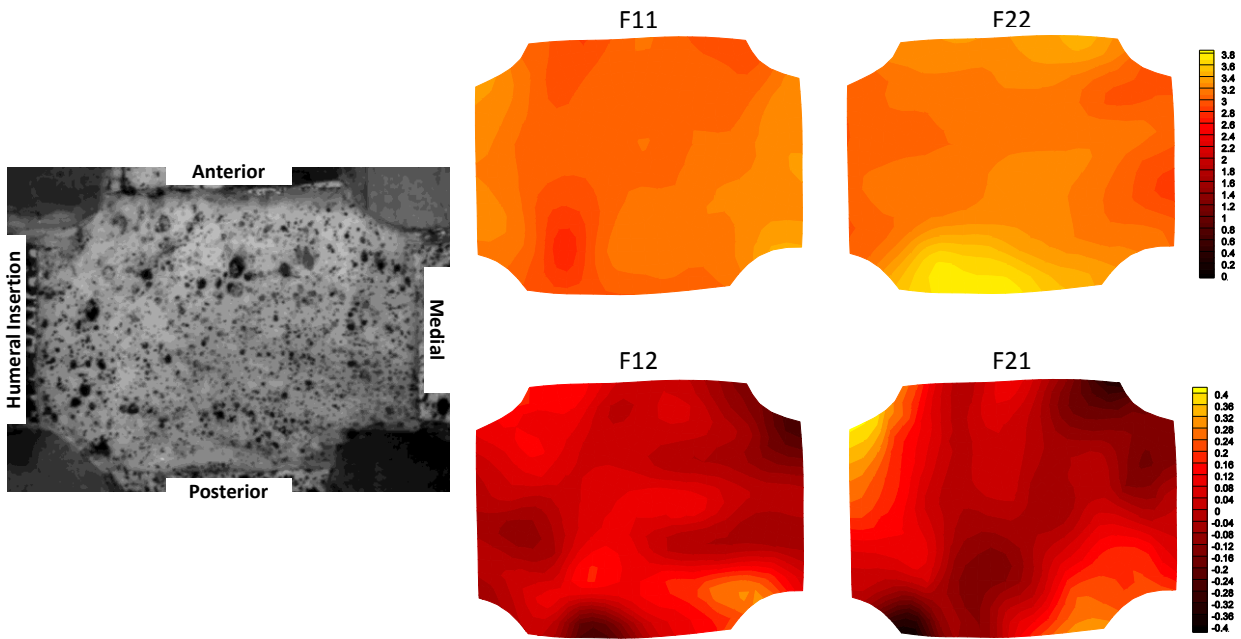


Fig. S3: Full-field deformation gradient tensor components for equibiaxial extension of supraspinatus tendon sample.

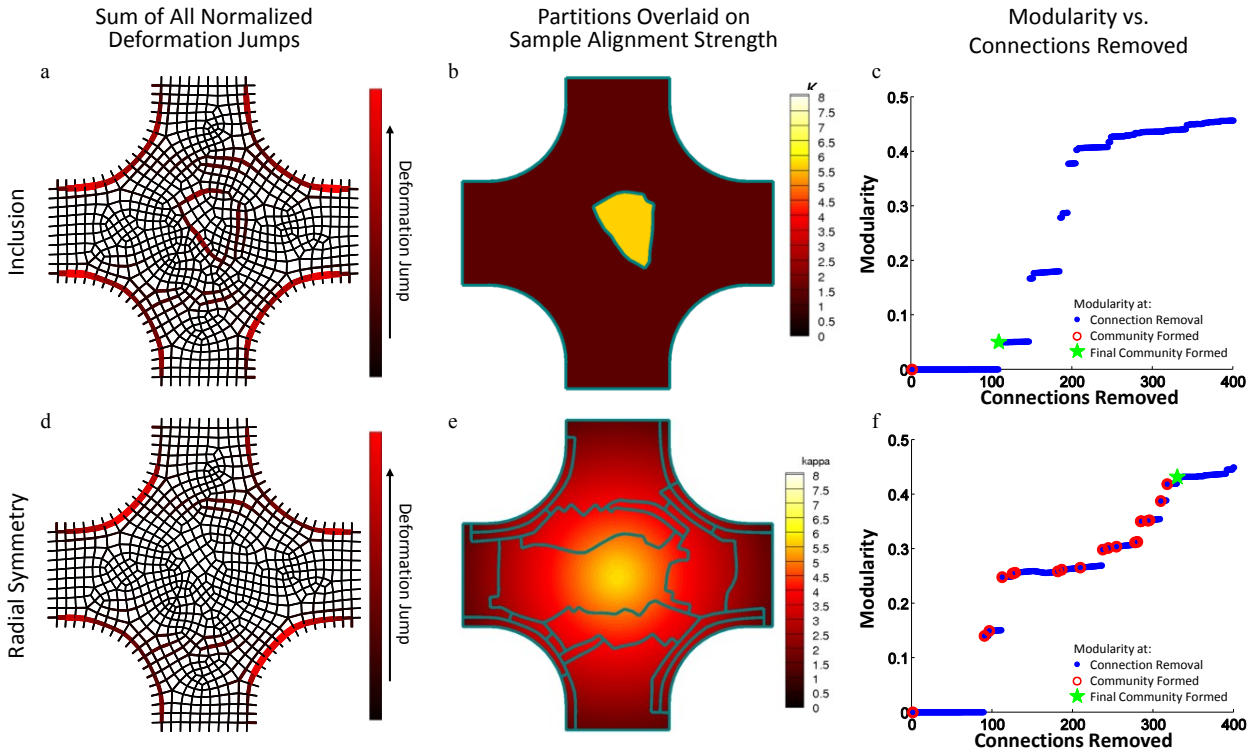


Fig. S4: Sum of normalized deformation gradient jumps for all three extensions for the simulated sample containing the inclusion with strength of alignment different from the bulk ( $\kappa_{bulk} = 1.5$  and  $\kappa_{inclusion} = 6.0$ ) (a) and for the radially aligned simulated sample with varied strength of alignment (d). Partitions, overlaid on sample geometry with contour map indicating strength of alignment, identified inclusion (b) and radial symmetry (e), respectively. Modularity as a function of connections removed for both the simulated sample containing the inclusion (c) and the radially aligned simulated sample (f). Blue dots indicate values when a connection is removed, open red circles indicate when a community is formed, and the green stars mark when the final community formed.

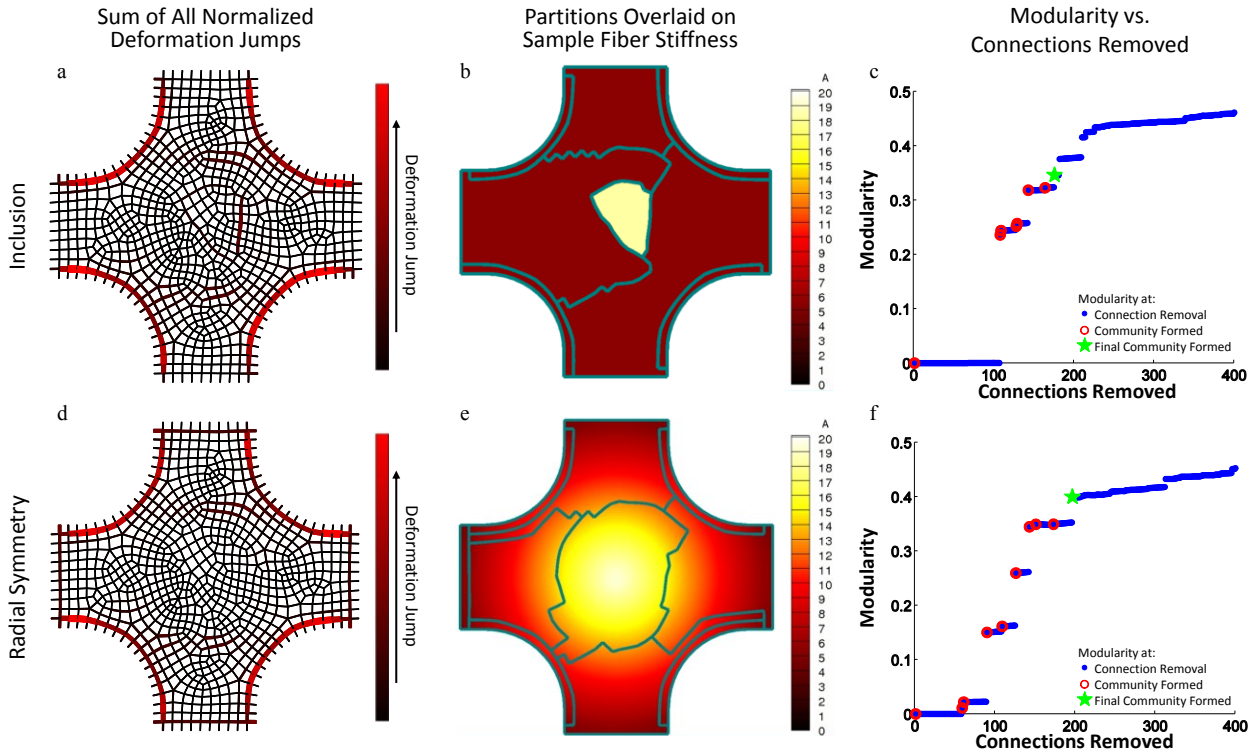


Fig. S5: Sum of normalized deformation gradient jumps for all three extensions for the simulated sample containing the inclusion with stiffness different from the bulk ( $A_{bulk} = 5 \text{ kPa}$  and  $A_{inclusion} = 20 \text{ kPa}$ ) (a) and for the radially aligned simulated sample with varied stiffness (d). Partitions, overlaid on sample geometry with contour map indicating stiffness, identified inclusion (b) and radial symmetry (e), respectively. Modularity as a function of connections removed for both the simulated sample containing the inclusion (c) and the radially aligned simulated sample (f). Blue dots indicate values when a connection is removed, open red circles indicate when a community is formed, and the green stars mark when the final community formed.

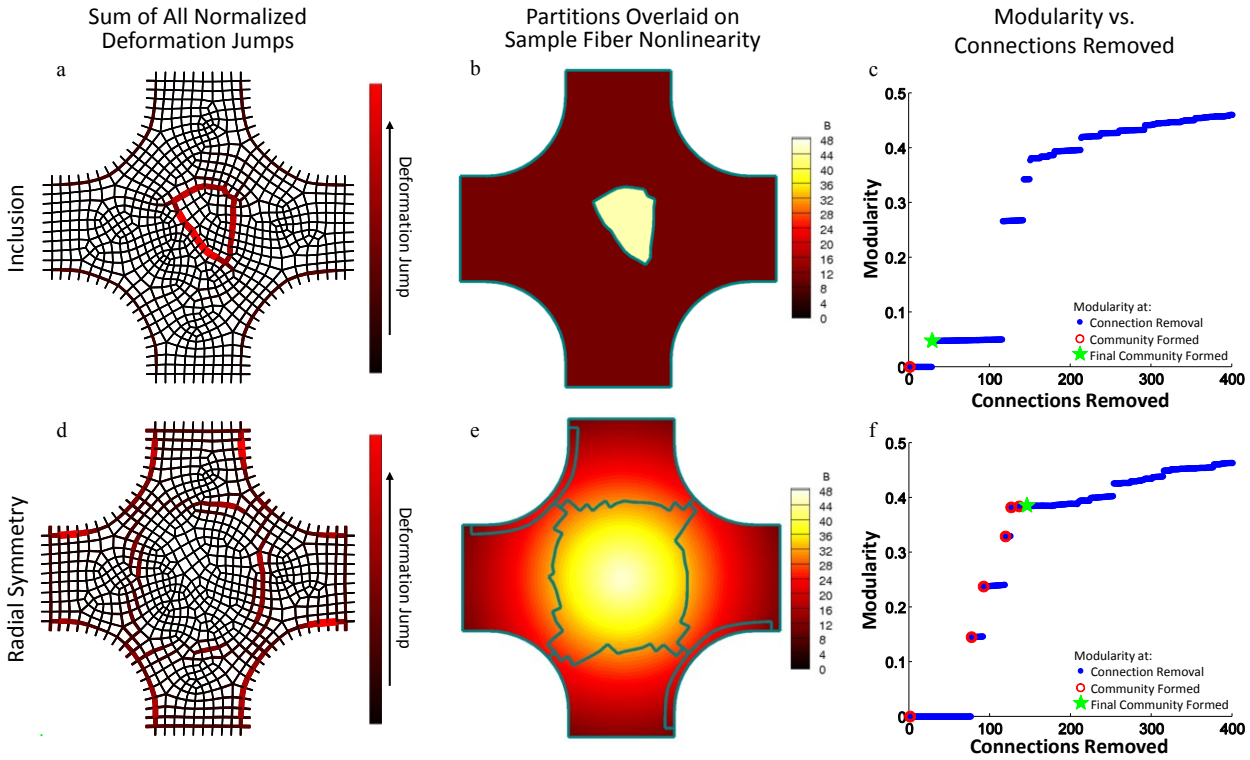


Fig. S6: Sum of normalized deformation gradient jumps for all three extensions for the simulated sample containing the inclusion with stiffness different from the bulk ( $B_{bulk} = 12$  and  $B_{inclusion} = 48$ ) (a) and for the radially aligned simulated sample with varied nonlinearity (d). Partitions, overlaid on sample geometry with contour map indicating nonlinearity, identified inclusion (b) and radial symmetry (e), respectively. Modularity as a function of connections removed for both the simulated sample containing the inclusion (c) and the radially aligned simulated sample (f). Blue dots indicate values when a connection is removed, open red circles indicate when a community is formed, and the green stars mark when the final community formed.

Video S1: Video of the cardiac sheet deformation overlaid with the partitioning results.

Partitioning Code is available in Matlab format.